Proposed "Congruent Matching Cells (CMC)" Method for Ballistic Identification and Error Rate Estimation

By: John Song, Physical Measurement Laboratory (PML), National Institute of Standards and Technology (NIST), Gaithersburg, MD 20899, U.S.A.; Phone: 301 975 3799; email: song@nist.gov

Keywords: ballistics identification, CMC, congruent matching cells, correlation cells, error rate, topography measurement

ABSTRACT

The 3D measurement and correlation on "correlation cells" were proposed at the National Institute of Standards and Technology (NIST) for establishing the NIST Ballistics Identification System (NBIS) [1]. Based on the concept of correlation cells, a Congruent Matching Cells (CMC) method is proposed for accurate ballistic identification and error rate estimation using three sets characteristic parameters of the paired correlation cells: cross correlation function maximum CCFmax, spatial registration positions in x-y and registration phase angle θ. The proposed CMC method can be used for correlation of both geometrical topographies and optical images. The "congruent matching" method can be potentially applied for all case scenarios of fired cartridge cases, fired bullets, and toolmarks. The CMC parameters and algorithms are in the public domain and subject to open tests. High-speed correlations are ensured by "synchronous processing" of multiple correlation cell pairs at the same time. Based on the CMC method, an error rate procedure is proposed for establishing a statistical foundation to support nationwide ballistics identifications in forensic science, and to provide an error rate report for court proceedings in a manner similar to the method used for reporting the Coincidental (Random) Match Probability (CMP) in forensic identification of DNA evidences.

Introduction

Side-by-side image comparisons using optical microscopes for ballistic identifications have more than a hundred-year history [2]. Since the late 1980s, different automated ballistics identification systems have been developed which typically include a digitized optical microscope, a signature analysis station and correlation software. Most of these systems are primarily based on comparisons of optical images acquired by microscopes under different lighting conditions. The correlation accuracy depends on image quality, which is largely affected by lighting conditions such as the type of light source, lighting direction, intensity, material color and reflectivity, and image contrast. Accurate identification also depends on the capability of the correlation software to identify the "valid correlation region" and to eliminate the "invalid correlation region" from correlation. Current commercial systems are using proprietary correlation parameters and algorithms to quantify image similarity without metrological traceability and objective open tests, which may make it difficult for laboratory assessments and interoperability among different systems. The lack of error rate estimation has been challenged when presenting evidence in court proceedings.

Ballistic signatures are a special kind of toolmark [3] and therefore, are geometrical surface topographies by nature. Direct measurements and correlations on surface topography have been proposed for ballistic identifications [4-7]. Since the 1980s, with the help of modern computer technology, different optical instruments have been developed that are capable of precise measurements of 3D surface topographies. These notably include confocal microscopes [8] and interference microscopes [9]. Such instruments have made it possible to use topography measurements for ballistic identification.

Since the late 1990s, NIST has developed Standard Reference Material (SRM) bullets and cartridge cases [10] which are being used as reference standards in crime laboratories in the United States and internationally. NIST has also developed a 2D/3D ballistics signature acquisition and correlation system [10] for certification measurements of the SRM bullets and cartridge cases to ensure the similarity of their topography signatures, as well as for experiments in ballistics identification. This system has produced matching accuracies for cartridge cases and bullets higher than those of a commercial system for all experiments thus far [11, 12].

A significant advancement at NIST is the recently proposed NIST Ballistics Identification System (NBIS) using 3D topography measurements on correlation cells [1]. Based on the concept of correlation cells, the Congruent Matching Cells (CMC) method is proposed for accurate ballistic identifications and error rate estimation. In this paper, basic concepts for correlation cells are introduced, followed by a discussion of the Congruent Matching Cells (CMC) method and a proposed error rate procedure.

Date Received: December 7, 2014
Peer Review Completed: December 9, 2014

Basic Concepts

Valid and Invalid Correlation Region

The correlated surfaces of fired bullets and ejected cartridge cases include valid and invalid correlation regions. The "valid correlation region" contains individual characteristics [3] of the ballistics signature that can be used effectively for identification. The "invalid correlation region" results from minimal interaction with gun parts during the firing process, and therefore does not contain individual characteristics of the ballistics signature and should be eliminated from consideration for identification.

Figure 1 demonstrates a correlation of two surface topographies, A and B, originating from the same firearm. The valid correlation region is represented by the superscript ($^+$); the invalid correlation region is represented by ($^-$). In **Figure 1**, the union symbol "∪" [13] is used to represent the union of two sets of images; the intersection symbol "∩" [13] is used to represent the intersection (or overlap) of two sets of images. For the individual topography A and B, each contains both the valid and invalid correlation regions (**Figure 1a**):

$$A = A^+ \cup A^-$$
$$B = B^+ \cup B^-$$
(1)

For a pair-correlated topography [A ∩ B] (**Figure 1b**):

$$[A \cap B] = [A^+ \cap B^+] \cup [(A^+ \cap B^-) \cup (A^- \cap B^+) \cup (A^- \cap B^-)],$$
(2)

where $[A^+ \cap B^+]$ represents the valid correlation region, $[(A^+ \cap B^-) \cup (A^- \cap B^+) \cup (A^- \cap B^-)]$ represents the invalid correlation region.

Correlation Cells

The correlation cell is designed for accurate ballistic identifications of 3D topography signatures. A correlation cell is a basic correlation unit with 1) a sufficiently small cell size so that a mosaic of cells can effectively represent the valid correlation region and separate it from the invalid correlation region; and 2) a sufficiently large cell size so as to contain a significant number of peaks and valleys for accurate topography correlations. Both are important for effective and accurate ballistic identifications. By using the correlation cells, the valid correlation region can be identified and the invalid correlation region can be eliminated from correlation. Thus the correlation accuracy can be increased.

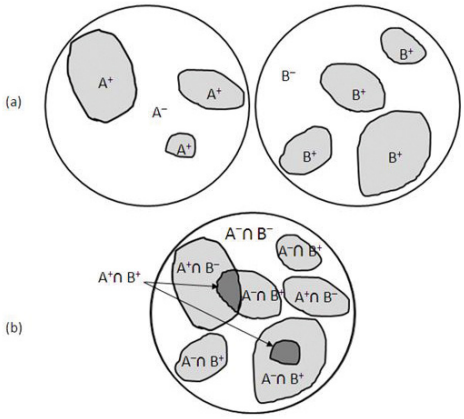

Figure 1: (a.) Valid correlation regions (A+ and B+) and invalid correlation region (A– and B–), for individual topographies A and B.

(b.) Common valid correlation regions [A+ ∩ B+] and invalid correlation regions [(A+ ∩ B-) ∪ (A- ∩ B+) ∪ (A- ∩ B-)] for a pair-correlated topography [A ∩ B].

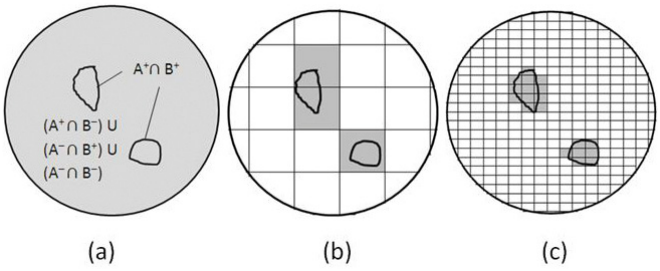

Figure 2: (a.) A pair of topographies [A ∩ B] correlated over the whole region, including both the valid and the invalid correlation regions.

(b.) Partial elimination of invalid correlation region and increase correlation accuracy.

(c.) Further elimination of invalid correlation region and increase of correlation accuracy through use of smaller correlation cells.

Figure 2a shows a pair-correlated topography [A ∩ B] including both valid correlation regions $[A^+ \cap B^+]$ (as shown by two inside encircled regions) and an invalid correlation region $[(A^+ \cap B^-) \cup (A^- \cap B^+) \cup (A^- \cap B^-)]$ (as shown by the remaining region). If the correlation is conducted in the whole region, the correlation accuracy represented by the cross correlation function maximum CCF_{max} [14] must be low,

because of the large invalid correlation region involved in the correlation (see **Figure 2a**). If the correlation region can be divided into correlation cells (see shadowed regions in **Figure 2b**), the cell correlations can be used for identifying the valid correlation regions and eliminating the invalid correlation regions; the correlation accuracy can thus be increased. If the cell size can be further reduced to a "sufficiently small" size but still contains "sufficiently large" topography information for ballistics identification (see shadowed regions in **Figure 2c**), the correlation accuracy can be further increased.

Cell Size

As stated previously, a correlation cell must be "sufficiently small" for high correlation accuracy; but must be "sufficiently large" to contain enough topography features for accurate ballistics identification. In other words, the cell size must be experimentally optimized; not too small and not too large. Either may result in low correlation accuracy.

The cell size also depends on the size and shape of the correlated topographies. If the correlation region is large and flat, such as the breech face impression of the cartridge cases, the cell size may be relatively large. If the correlation region is small and contains curvatures, such as the firing pin impression, or if the correlated region contains complex shapes, such as some ejector mark impressions and damaged bullets, the cell size may necessarily be smaller.

As a starting point for testing of the 9 mm caliber cartridge cases, it is estimated that the cell size for breech face correlations be in the range of (0.25 mm × 0.25 mm) to (0.5 mm × 0.5 mm). Those estimates imply that the number of cells is in the range of about 50 to 200 for the correlations of breech face of 9 mm cartridge cases.

Identification of the Valid and Invalid Correlation Regions Using Correlation Cells

If topographies A and B, originating from the same firearm, are registered at their maximum correlation position (**Figure 3**), the registered cell pairs located in their common valid correlation regions (as shown by the solid cell pairs A_1, A_2, A_3… and B_1, B_2, B_3…) are necessarily characterized by [1]:

1) High pairwise topography similarity quantified by the cross correlation function maximum CCF_{max} [14];

2) Similar registration angles θ for all correlated cell pairs in topography A and B; and

3) A "Congruent" *x-y* spatial distribution pattern for the correlated cell arrays A_1, A_2, A_3… and B_1, B_2, B_3… or nearly so.

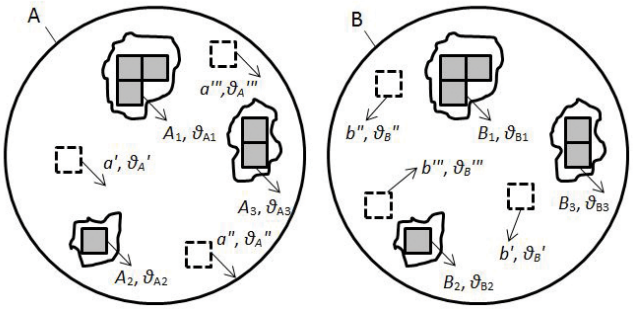

Figure 3: Assuming A and B originated from the same firearm, there are three sets of correlation cells A1, A2, A3 and B1, B2, B3 located in three valid correlation regions [A+ ∩ B+] (as shown by three inside encircled regions). The other cell pairs a', a", a'"… and b', b", b'"… are located in the invalid correlation region [(A+ ∩ B-) ∪ (A- ∩ B+) ∪ (A- ∩ B-)] (as shown by the remaining region). Correlation cells in topography A are used as reference cells for correlation with cells arrays in topography B.

On the other hand, if the registered cell pairs come from the invalid correlation regions of A and B (such as the dotted cells *a'*, *a"*, *a'"*… and *b'*, *b"*, *b'"*… in **Figure 3**), or if the samples originated from different firearms, their cross correlation value CCF_{max} would be relatively low, and their cell arrays would show significant difference in *x-y* distribution patterns and registration angles θ.

The Proposed "Congruent Matching Cells (CMC)" Method

The "Congruent Matching Cells (CMC)" Method

Congruent matching cell pairs, or CMCs, are therefore determined by three sets of identification parameters: cross correlation value CCF_{max}, registration angle θ, and translation distances in x and y with corresponding thresholds T_{CCF}, T_θ, T_x and T_y. The correlated cell pairs are considered CMCs—that is, part of a congruent matching cell pattern—when their correlation value CCF_{max} is greater than a chosen threshold T_{CCF} and their registration angle θ and x, y registration positions are within the chosen threshold limits T_θ, T_x and T_y.

How many CMC pairs are required so that the overall surface topographies can be identified as matching? As a starting point, we use a numerical identification criterion *C*

equal to 6, taking a lead from the method of Consecutively Matching Striae (CMS) developed by Biasotti and Murdock for identification of bullet striation signatures [15-17]. This method has been used internationally for bullet and striated toolmark identifications since 1984 [16]. As a starting point for tests, the numerical criterion for Consecutively Matching Striae (CMS) method, C = 6, is adopted for the proposed Congruent Matching Cells (CMC) method:

> *At least C (assuming C = 6 as a start point for test) Congruent Matching Cell (CMC) pairs show high correlation values represented by* $CCF_{max} \geq T_{CCF}$*; show the "congruent" distribution pattern represented by the same spatial x-y registration positions within the threshold* T_x *and* T_y*, and show the same registration phase angle* θ *within the threshold* T_θ*.*

Validation Tests for the Proposed CMC Method

An initial validation test of the CMC method was conducted using a set of cartridge cases obtained from a study initiated by the Miami-Dade Crime Laboratory using consecutively manufactured pistol slides [18]. Ballistic correlations using consecutively manufactured gun parts represent the most critical scenario for testing the capability to identify bullets or cartridge cases fired or ejected from the same firearm. Accordingly, 40 cartridge cases ejected from handguns with 10 consecutively manufactured pistol slides were obtained from that study. The impression topographies of the pistol slides on the cartridge cases were measured by a confocal microscope [8], and these signatures were correlated by the CMC method. A total of 780 correlations were performed for the validation tests, comprising 63 known matching (KM) and 717 known non-matching (KNM) correlations [19].

Validation tests showed that there was a significant separation between CMC distributions of the KM and KNM samples without an overlap [19]. Additional tests conducted using different correlation parameters and slightly different versions of the correlation software also show similar results without an overlap [19]. These correlation results strongly support the CMC method and the numerical identification criterion C = 6 for firearm identifications. The identification accuracy can likely be further improved by optimization of the number of cells and the settings for the correlation parameters, and by using finer registration intervals. Similar validation tests performed using 780 optical intensity image pairs of the same set of 40 cartridge cases, instead of using 3D geometrical topographies, also show similar results without any false identifications or false exclusions [20].

Proposed Error Rate Procedure Based on the CMC Method

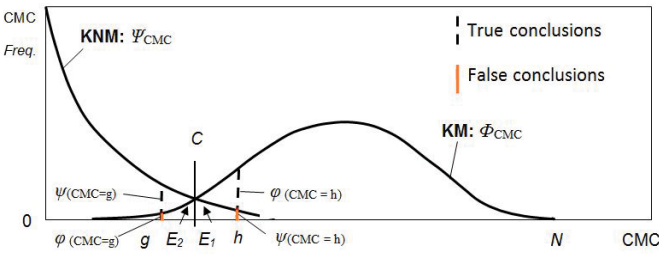

Figure 4: A conceptual model for CMC distributions, Φ_{CMC} and Ψ_{CMC}, of paired KM and KNM topographies.

As mentioned previously, side-by-side toolmark image comparisons for ballistic identification have more than a hundred-year history [1]. However, the scientific foundation of firearm and toolmark identification has been challenged by recent court decisions. As stated in a 2008 National Academies Report [21]:

> *The validity of the fundamental assumptions of uniqueness and reproducibility of firearms-related toolmarks has not yet been fully demonstrated…recent court decisions in which admissibility of firearms toolmark evidence was in question have generally accepted that the field has validity but have refused to accept 'exclusion of all other firearms' arguments… Since the basis of all forensic identification is probability theory, examiners can never really assert a conclusion of an 'identification to exclusion of all others in the world,' but at best can only assert a very small (objective or subjective) probability of a coincidental match…*

These statements were emphasized once again in a 2009 NRC report [22]. The legal standard for acceptance of scientific evidence contained in the U.S. Supreme Court decision, called the *Daubert* standard [22], "*places high probative weight on quantifiable evidence that can be tested empirically and for which known or potential error rates may be estimated, such as identification using DNA markers* [22]." It has been a national priority in forensic science to establish a scientific procedure for quantitative error rate reports to support firearm identifications in court proceedings, in a manner similar to the method used for reporting the Coincidental (Random) Match Probability (CMP) in forensic identification of DNA evidence.

False Positive and False Negative Error Rate E_1 and E_2

Figure 4 shows a conceptual model for CMC distribution density functions, Φ_{CMC} and Ψ_{CMC}, of KM and KNM

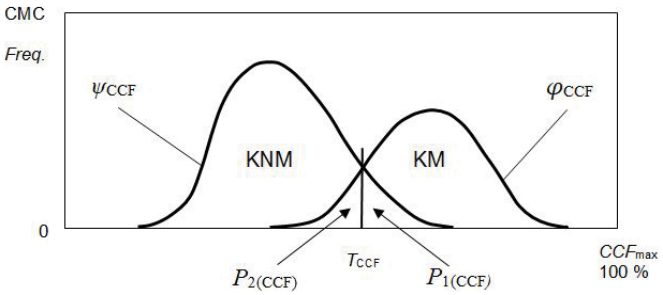

Figure 5: A conceptual model of CMC frequency distribution, φ_{CCF} and ψ_{CCF}, for correlation parameter CCF_{max} of the KM and KNM topography pairs.

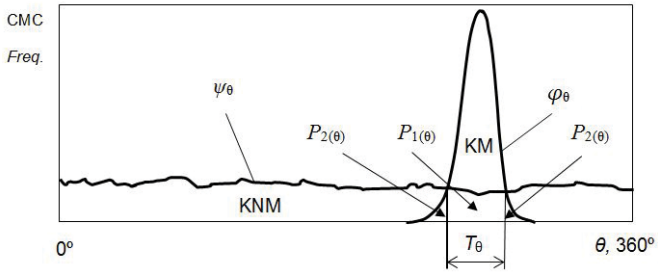

Figure 6: A conceptual model of CMC frequency distribution for correlation parameter θ of the KM and KNM topography pairs.

topography pairs, respectively. Both the Φ_{CMC} and Ψ_{CMC} distribution can be modeled by Binomial distribution [23] for error rate estimation (to be discussed later). The CMC distribution of KM and KNM topography pairs may be separated without an overlap if there is only a limited sample size [19, 20]. However, they may have an overlap if the sample size is large enough (see the conceptual model in **Figure 4**). When the numerical identification criterion C is selected at the intersect region (see **Figure 4**), the KM topography pairs may be missed identifications as "Non-match," or "false negative" error E_2; the KNM topography pairs may be misidentified as "Match," or "false positive" error E_1. Accordingly, the numerical criterion C can be determined by the acceptable false positive and false negative error rate E_1 and E_2. If E_1 and E_2 are too large to be accepted, different numerical identification criteria C_{HIGH} and C_{LOW} may be defined for the determination of "Match" and "Non- match", i.e., when CMC $\geq C_{HIGH}$, it is concluded as a "Match"; when CMC $< C_{LOW}$, it is concluded as a "No-match." When the CMC numbers are between C_{HIGH} and C_{LOW}, it is concluded as "No-conclusion" which needs further accurate correlations.

The CMC method using three sets of identification parameters for uniquely identifying correlated cell pairs originating from the same firearm enables an approach to estimating error rates based on statistical analysis of the total numbers of effective correlation cells N, the numerical identification criterion C, and the statistical distributions of the three sets of identification parameters, from which the combined false positive and false negative identification probability for each correlated cell pairs, P_1 and P_2, can be calculated for the error rate estimation. This is discussed in the following sub-sections.

Determination of CMC Distributions for the Three Sets of Identification Parameters

CMC Distribution of the Parameter CCF_{max}

Figure 5 shows a conceptual model of CMC frequency distribution for correlation parameter CCF_{max} of the KM and KNM topography pairs, φ_{CCF} and ψ_{CCF}, represented by the frequency density of the CMC distribution in the range of CCF_{max} from zero to 100 %. Assuming the distribution patterns of both φ_{CCF} and ψ_{CCF} are close to Gaussian distribution (this assumption has been verified by experimental tests [19, 20]). There may be an overlap between the CMC distributions of CCF_{max} parameter for KM and KNM topographies if the sample size is large enough (see **Figure 5**), which represents the false positive and false negative identification probability, $P_{1(CCF)}$ and $P_{2(CCF)}$, for the correlated cell pairs caused by the threshold T_{CCF} of the identification parameter CCF_{max}. $P_{1(CCF)}$ and $P_{2(CCF)}$ will be combined with the other two uncertainty components caused by the other two sets of identification parameters, θ and x-y, as the combined false positive and false negative identification probability for the correlated cell pairs, P_1 and P_2, for calculations of the false positive and false negative error rate E_1 and E_2.

CMC Distribution of the Parameter θ

Figure 6 shows a conceptual model of CMC frequency distribution, φ_θ and ψ_θ, for correlation parameter θ of the KM and KNM topography pairs, represented by the frequency density of the CMC distribution in the range of θ from zero to 360°. For the KM topographies, the CMC distribution pattern φ_θ may be close to a Gaussian distribution. For the KNM topographies, however, the CMC distribution pattern ψ_θ may be close to a uniform distribution (this assumption has been verified by experimental tests [19, 20]). When the threshold of T_θ (see **Figure 6**) is used for the determination of the "congruent cell pairs," there are overlaps between these two distribution curves φ_θ and ψ_θ. The overlaps represent the false positive and false negative identification probabilities, $P_{1(\theta)}$ and $P_{2(\theta)}$, for the correlated cell pairs caused by θ, which will cause misidentifications (or false positive error) E_1, and

missed identifications (or false negative error) E_2.

CMC Distribution of the Parameter *x* and *y*

Similarly, **Figure 7** shows a conceptual model of CMC frequency distribution, $\varphi_{(xy)}$ and $\psi_{(xy)}$, for correlation parameter *x* and *y* of the KM and KNM topography pairs, represented by the frequency density of the CMC distribution in the whole registration range of *x* and *y*. For the KM topographies, the CMC distribution pattern $\varphi_{(xy)}$ may be close to a Gaussian distribution. For the KNM topographies, however, the CMC distribution pattern $\psi_{(xy)}$ may be close to a uniform distribution (this assumption has also been verified by experimental tests [19, 20]). When the threshold of T_x and T_y (see **Figure 7**) are used for the determination of the "congruent cell pairs," there are overlaps between these two distribution curves $\varphi_{(xy)}$ and $\psi_{(xy)}$, which represent the false positive and false negative identification probabilities $P_{1(x,y)}$ and $P_{2(x,y)}$ for the correlated cell pairs caused by *x* and *y* registrations. $P_{1(x,y)}$ and $P_{2(x,y)}$ will also cause misidentifications (or false positive error) E_1, and missed identifications (or false negative error) E_2.

The Combined False Positive and False Negative Identification Probability P_1 and P_2

As stated before, both the false positive and false negative error rate E_1 and E_2 can be calculated by the total cell number *N*, the numerical identification criterion *C* (we use *C* = 6 for initial study) and the combined false positive and false negative identification probability for each correlated cell pairs, P_1 and P_2, which are estimated by a statistical combination of the individual false positive and false negative identification probabilities associated with the three sets of identification parameters CCF_{max}, θ, *x* and *y*. This calculation must consider cross-correlation effects between the three sets of identification parameters. For the finite data set here, it is suggested to take an experimental approach to deriving P_1 and P_2 by estimating conditional probabilities one parameter at a time. First, the number of KNM cell pairs that pass the T_{CCF} threshold are counted and compared with the total number of correlated cell pairs to derive the individual false positive identification probability $P_{1(CCF)}$. Then only the cell pairs passing the T_{CCF} test are included in the probability distribution for the next test of parameter θ, from which the conditional false positive identification probability $P_{1(\theta|CCF)}$ is estimated, and so on.

Based on the "conditional probability test method", the combined identification probabilities P_1 and P_2 can be estimated as the product of the conditional experimental identification probabilities associated with each individual identification parameter. The combined false positive identification probability P_1 for each correlated cell pairs of the KNM topography is defined as the probability that all four individual identification parameters are incorrectly showing positive, that is, the CCF_{max} result is above the threshold T_{CCF} and the three spatial parameters are within the chosen threshold limits T_θ, T_x and T_y. As a result, P_1 can be estimated by:

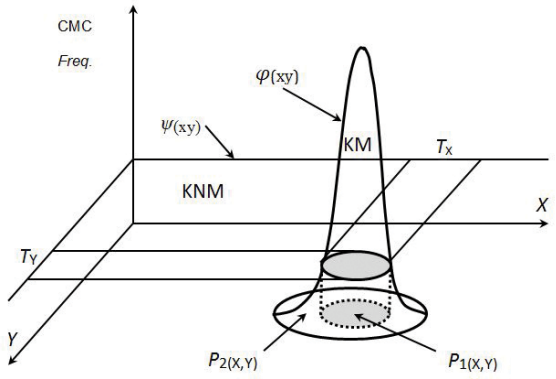

Figure 7: A conceptual model of CMC frequency distribution for correlation parameter *x* and *y* of the KM and KNM topography pairs.

$$P_1 = \prod_{i=1}^{i=4} P_{1(i)}$$

$$= P_{1(CCF)} \times P_{1(\theta|CCF)} \times P_{1(x|\theta,CCF)} \times P_{1(y|x,\theta,CCF)} \quad (3a)$$

On the other hand, the combined false negative identification probability P_2 for each correlated cell pair of the KM topography is defined as the probability that any of the three sets identification parameters (and/or their combinations) incorrectly yields an "uncorrelated" result, which means that the parameter value is out of the range of the T_{CCF} threshold or spatial threshold limits T_θ, T_x and T_y. As a result, P_2 can be estimated by:

$$P_2 = 1 - \prod_{i=1}^{i=4} [1 - P_{2(i)}]$$

$$= 1 - [(1 - P_{2(CCF)}) \times (1 - P_{2(\theta|CCF)}) \times (1 - P_{2(x|\theta,CCF)}) \times (1 - P_{2(y|x,\theta,CCF)})] \quad (3b)$$

Based on the distribution functions and thresholds of the three

sets of identification parameters, CCF_{max}, θ and x-y, their false positive and false negative identification probabilities $P_{1(CCF)}$, $P_{1(\theta)}$, $P_{1(xy)}$, and $P_{2(CCF)}$, $P_{2(\theta)}$, $P_{2(xy)}$ can be determined, from which the combined false positive and false negative identification probability P_1 and P_2 can be calculated by Eq. 3a and 3b for calculation of the false positive and false narrative error rates E_1 and E_2.

Statistical Error Rate Estimation

Cumulative False Positive Error Rate E_1

The sub-false positive error rate $e_{1(CMC=h)}$ caused by the ballistic identifications with the specific CMC number h (see **Figure 4**, h is within the range of $C \le h \le N$) can be calculated by the Binomial distribution (N, P_1) [23]:

$$\psi_{(CMC=h)} = C_N^h \cdot (P_1)^h \cdot (1 - P_1)^{N-h} \quad (4)$$

The cumulative false positive error rate E_1 is given by the sum of the discrete probability mass function $e_{1(CMC)}$ with CMC values between C and N:

$$E_1 = \sum_{CMC=C}^{CMC=N} e_{1(CMC)} = e_{1(CMC=C)} + e_{1\,(CMC=C+1)} + \cdots + e_{1(CMC=N)}$$
$$= \psi_{(CMC=C)} + \psi_{(CMC=C+1)} + \cdots + \psi_{(CMC=N)}$$
$$= 1 - (\psi_{(CMC=0)} + \psi_{(CMC=1)} + \cdots + \psi_{(CMC=C-1)}). \quad (5)$$

Where E_1 is the cumulative false positive error rate which is determined by three factors: N is cell number, C is the numerical identification criterion of CMC method (assuming $C = 6$ at this point); P_1 is the combined false positive identification probability of the CMC method calculated from Eq. 3a. C_N^h stands for the number of ways of choosing h elements out of total N elements without repeating.

Cumulative False Negative Error Rate E_2

The sub-false negative error rate $e_{2(CMC=g)}$ caused by the ballistic identifications with the specific CMC number g (see **Figure 4**, g is within the range of $0 \le g \le C - 1$) can also be calculated by the Binomial distribution (N, $1 - P_2$) [23]:

$$\varphi_{(CMC=g)} = C_N^g \cdot (1 - P_2)^g \cdot (P_2)^{N-g} \quad (6)$$

The cumulative false negative error rate E_2 is the sum of the discrete probability mass function $e_{2(CMC)}$ with CMC values between 0 and $(C - 1)$:

$$E_2 = \sum_{CMC=0}^{CMC=C-1} e_{2\,(CMC)} = e_{2\,(CMC=0)} + e_{2\,(CMC=1)} + \cdots + e_{2\,(CMC=C-1)}$$
$$= \varphi_{(CMC=0)} + \varphi_{(CMC=1)} + \cdots + \varphi_{(CMC=C-1)} \quad (7)$$

Where E_2 is the false negative error rate which is also determined by three factors: cell number N, the numerical identification criterion C, and the combined false negative identification probability P_2 calculated from Eq. 3b. Whenever the three factors are determined by experimental tests and statistical analysis, the false negative error E_2 can be calculated.

The Individual False Identification and False Exclusion Error Rate R_1 and R_2

Figure 4 also illustrates the probabilities of true and false conclusions by the dotted bars and the solid bars for specific CMC values, h and g. These probabilities (R_1 and R_2) can be compared in likelihood ratios [24]. In this report, they are utilized to estimate two other key parameters, the individual false identification and false exclusion error rates R_1 and R_2, defined as the division of the probability of possible false conclusions (the solid bars in **Figure 4**) by the sum of the probabilities of both the false (the solid bars) and the true conclusions (the dotted bars), each given their respective probability models, and calculated for specific CMC values of h and g. The individual false identification error rate R_1 represents the estimated probability that a topography pair classified as "matching" with a specific CMC number h ($h \ge C = 6$) is in fact a non-matching pair, or it is actually fired from different guns. It can be estimated by:

$$R_{1(CMC=h)} = \frac{K \times \psi_{(CMC=h)}}{K \times \psi_{(CMC=h)} + \varphi_{(CMC=h)}} \quad (h \ge C = 6), \quad (8)$$

where K is the ratio of the population size of KNM to KM topography pairs. The individual false exclusion error rate R_2 represents the estimated probability that a topography pair classified as "non-matching" with a specific CMC number g ($g < C = 6$) is actually a KM topography pair mistakenly classified. It can be estimated by:

$$R_{2(CMC=g)} = \frac{\varphi_{(CMC=g)}}{\varphi_{(CMC=g)} + K \times \psi_{(CMC=g)}} \quad (g < C = 6) \tag{9}$$

R_1 and R_2 could provide a support to ballistics examiners at court proceedings if they were asked questions such as "when concluding the two evidence samples are fired from the same firearm, what is the probability if they are actually fired from different firearms (false identification probability R_1)?" Or "when concluding the two evidence samples are fired from different firearms, what is the probability if they are actually fired from the same firearm (false exclusion probability R_2)?"

Determination of the thresholds T_{CCF}, T_θ, T_x and T_y

The thresholds T_{CCF}, T_θ, T_x and T_y can be determined by experimental tests and statistical analyses for a large number correlations of known-matching (KM) and known-non-matching (KNM) samples. It must be noted that the selection of thresholds T_{CCF}, T_θ, T_x and T_y will affect the ratio of the three sets of individual false positive and false negative identification probabilities: $P_{1(CCF)}$ vs. $P_{2(CCF)}$, $P_{1(\theta)}$ vs. $P_{2(\theta)}$ and $P_{1(xy)}$ vs. $P_{2(xy)}$. As a result, it will affect the ratio of combined false positive and false negative identification probability P_1 vs. P_2, as well as the ratio of false positive and false negative error E_1 vs. E_2. Therefore, the selection of thresholds T_{CCF}, T_θ, T_x and T_y must be well balanced between the ratio of false positive and false negative error rates E_1 and E_2.

Initial error rate estimation results

Based on the proposed error rate procedure, initial error rate estimation has been recently completed using a set of initial validation test samples with 40 cartridge cases ejected from handguns with 10 consecutively manufactured pistol slides [18, 19]. That includes 780 pair-wise correlations comprising 63 known matching (KM) and 717 known non-matching (KNM) correlations. Test results have shown that the experimental CMC distributions for the KM and KNM topographies are close to the theoretical distribution (see **Figure 4**); and the experimental CMC distributions for the three sets of correlation parameters CCF_{max}, θ and x, y of the KM and KNM topographies are also close to the theoretical distributions (see **Figures 5, 6 and 7**). Based on these statistical distributions, the combined false positive and false negative identification probability P_1 and P_2 are calculated, from which the cumulative false positive and false negative error E_1 and E_2 and the individual false identification and false exclusion error rates R_1 and R_2 are estimated [25]. All the estimated error rate values are within an "extremely strong level" of the likelihood ratio for admission of evidence in court proceedings (10^{-6} or less) [24]. The initial error rate estimation results will be published soon [25].

Summary

The Congruent Matching Cells (CMC) method is proposed for accurate ballistics identification and error rate estimation. The CMC method is based on correlation of pairs of small correlation cells instead of correlation of the entire sample images. Three sets of identification parameters are devised for uniquely identifying correlated cell pairs originating from the same firearm. This enables an approach to estimating error rates based on statistical analysis of the total numbers of correlation cells, the numerical identification criterion and the statistical distribution of the three sets of identification parameters. Validation tests using the CMC method have not produced any false identifications or false exclusions. A statistical procedure for estimating error rates has been developed. The estimated false positive and false negative error rates are within an "extremely strong level" of the likelihood ratio for admission of evidence in court proceedings (10^{-6} or less) [24]. The proposed CMC method has established a statistical foundation to support nationwide ballistics identifications in forensic science, and to provide error rate reports for court proceedings in a manner similar to the method for reporting the Coincidental (Random) Match Probability (CMP) in forensic identification of DNA evidences.

The proposed CMC method and error rate procedure may also serve as a foundation for manufacturers to develop next generation ballistic identification systems characterized by high correlation accuracy and error rate reporting, which would represent a decided advance over current automated ballistic identification systems. An error rate procedure could also be used for laboratory assessment and accreditation in accordance with the ISO 17025 standard [26] and ASCLD/LAB procedures [27].

Acknowledgements

The funding for this research is provided by NIST's Forensic Measurements Challenge Program (FMC2012) and by the Special Programs Office (SPO) at NIST. The author is grateful to T.V. Vorburger, W. Chu, J. Yen, R.M. Thompson, and S.M. Ballou of NIST for their discussion, review, and comments. The author is also grateful to T. Fadul of the Miami Dade

Crime Lab. and A. Zheng of NIST for providing test samples and topography data.

References

[1] Song, J., "Proposed NIST Ballistics Identification System (NBIS) using 3D Topography Measurements on Correlation Cells," AFTE Journal, Vol. 45, No. 2, 2013, pp. 184-189.
[2] Hamby, J., "The History of Firearm and Toolmark Identification," AFTE Journal, Vol. 31, No. 3, 1999, revised 2008.
[3] "The Theory of Identification, Range of Striae Comparison Reports and Modified Glossary Definitions – An AFTE Criteria for Identification Committee Report," AFTE Journal, Vol. 24, No. 3, 1992, pp. 337.
[4] De Kinder, J., Bonfanti, M., "Automated Comparisons of Bullet Striations Based on 3D Topography," Forensic Science International, Vol. 101, No. 2, 1999, pp. 85-93.
[5] Song, J., Vorburger, T. V., "Topography Measurement and Applications," in Proc. SPIE -The 3rd International Symposium on Precision Mechanical Measurements, SPIE 6280: 1T1-1T8, SPIE, Bellingham, WA, 2006.
[6] Song, J., Vorburger, T.V., Ballou, S., Thompson, R., Yen, R., Renegar, T.B., Zheng, A., Silver, R., Ols, M., "The National Ballistics Imaging Comparison (NBIC) Project," Forensic Science International, Vol. 216**,** pp. 168-182, 2012, online publication at: http://dx.doi.org/10.1016/j.forsciint.2011.09.016.
[7] Song, J., Chu, W., Vorburger, T.V., Thompson, R., Yen, J., Renegar, T.B., Zheng, A., Silver, R., "Development of Ballistic Identifications – From Image Comparison to Topography Measurement in Surface Metrology," Measurement Science and Technology, Vol. 23**,** No. 4, 2012, online publication at: http://stacks.iop.org/0957-0233/23/054010.
[8] Hamilton, D.K., Wilson, T., "Three-dimensional Surface Measurement Using the Confocal Scanning Microscope," Applied Physics, Vol. 27, No. 4, 1982, pp. 211-213.
[9] Wyant, J.C., Koliopoulos, C.L., Bhushan, B., Basila, D., "Development of a Three-dimensional Noncontact Digital Optical Profiler," Journal of Tribology. Vol. 108, No. 1, 1986, pp. 1-8.
[10] Song, J., Whitenton, E., Kelley, D., Clary, R., Ma, L., Ballou, S., "SRM 2460/2461 Standard Bullets and Cartridge Cases Project," Journal of Research of NIST, Vol. 109**,** No. 6, 2004, pp. 533-542.
[11] Vorburger, T.V., Yen, J., Bachrach, B., Renegar, T.B., Filliben, J., Ma, L., Rhee, L.H., Zheng, A., Song, J., Riley, M., Foreman, C., Ballou, S., Surface Topography Analysis for a Feasibility Assessment of a National Ballistics Imaging Database, NISTIR 7362, National Institute of Standards and Technology, 2007.
[12] Chu, W., Song, J., Vorburger, T.V., Yen, J., Ballou, S., Bachrach, B., "Pilot Study of Automated Bullet Signature Identification Based on Topography Measurements and Correlations," Journal of Forensic Sciences, Vol. 55, No. 2, 2010, pp, 341-347.
[13] ISO 80000-2, "Qualities and units – Part 2: Mathematical signs and symbols to be used in the natural sciences and technology," ISO, 2009.
[14] Song, J., Vorburger, T.V., "Proposed Bullet Signature Comparisons Using Autocorrelation Functions," Proc. 2000 NCSL, NCSL-International, Toronto, 2000.
[15] Biasotti A.A., "A Statistical Study of the Individual Characteristics of Fired Bullets," Journal of Forensic Science, Vol. 4, 1959, pp. 34-50.
[16] Biasotti, A.A., Murdock, J.E., "Criteria for Identification or State of the Art of Firearm and Toolmark Identification," AFTE Journal, Vol. 16, No. 4, 1984.
[17] Biasotti, A., Murdock, J., and Moran, B. Chapter 35 "Firearms and Toolmark Identification," pp. 641-730 in Vol. 4, Modern Scientific Evidence: The Law and Science of Expert Testimony, 2011-2012 Edition (Faigman, DL, Blumenthal, JA, Sanders, J, Chen, EK, Mnookin, JK, and Murphy, EE.), Eagan, MN: Thompson-Reuters/West, p. 690.
[18]Fadul, T., "An Empirical Study to Improve the Scientific Foundation of Forensic Firearm and Tool Mark Identification Utilizing 10 Consecutively Manufactured Slides," Department of Justice, Award Number 2009-DN-BX-K230, 2009.
[19]Chu, W., Tong, M., Song, J., "Validation Tests for the Congruent Matching Cells (CMC) Method Using Cartridge Cases Fired with Consecutively Manufactured Pistol Slides," AFTE Journal, Vol. 45, No. 4, 2013, pp. 361-366.
[20]Tong, M., Song, J., Chu, W., Thompson, R.M., "Fired Cartridge Case Identification Using Optical Images and the Congruent Matching Cells (CMC) Method," Journal of Research of the National Institute of Standards and Technology, Vol. 119, 2014, pp. 575-582. http://dx.doi.org/10.6028/jres.119.023.
[21]Ballistic Imaging, National Research Council, 3, 82, 20, 2008.
[22]Strengthening Forensic Science in the United States--A Path Forward, National Research Council, 5-20, 6-2 (2009).
[23]Ross, S., A First Course in Probability, MacMillan, New York, 1976.
[24]Liebscher, T., "Firearm Identification with Bayes?" ENFSI Expert Working Group Firearms/GSR 2013 Annual Meeting, Riga, (2013).
[25]Song, J., Vorburger, T.V., Chu, W., Yen, J., Soons, J.A., D.B. Ott, Zheng, A., "Estimating Error Rates for Firearm Evidence Identifications in Forensic Science," passed NIST review, to be submitted for publication.
[26]ISO 17025, ISO, Geneva, 2005.
[27]American Society of Crime Laboratory Directors / Laboratory Accreditation Board (ASCLD/LAB), http://www.ascld.org.